

Multi-Reggeon Behavior of Production Amplitudes

I. T. DRUMMOND

Department of Applied Mathematics and Theoretical Physics, University of Cambridge, England

(Received 24 April 1968; revised manuscript received 16 July 1968)

Gribov's approach is used to investigate the asymptotic properties of production amplitudes. When it is applied to an analysis of double Reggeon exchange, the results of previous authors are confirmed. In particular, it is verified that the amplitude $f_{\alpha_1\alpha_2}$ for the coupling of two Reggeons, α_1 and α_2 , to a particle (of mass M) depends not only on the masses $q_1'^2$ and $q_2'^2$ of the Reggeons, but also on $q_3'^2 = (q_1' - q_2')^2$. (Primed vectors are spacelike and perpendicular to the incident beam.) On the basis of a diagrammatic model, the dependence of $f_{\alpha_1\alpha_2}$ on $q_3'^2$ is elucidated. When $M = m_\pi$, a strong variation of $f_{\alpha_1\alpha_2}$ throughout the physical region is expected. The same approach is applied to an analysis of a Reggeon triangle graph. Gribov's rules are found to apply provided that certain extra factors are included in the integrand. Because of these factors, the Reggeon "Ward identity" suggested by Anselm and Dyatlov no longer holds. The analytic structure of the corresponding double partial-wave amplitude is investigated. It has ordinary two-Reggeon singularities in each angular momentum separately, together with a leading curve depending on both variables. For the triangle graph, it turns out that the leading curve determines the asymptotic behavior, which is of the form $s^J/\ln s$, where the exponent J depends on $q_3'^2$ as well as on $q_1'^2$ and $q_2'^2$. This type of behavior has no analog in two-body scattering, and it would be of interest to identify such behavior experimentally. Finally, it is pointed out that underlying the definition of the approximate double partial wave used in this paper is the asymptotic simplicity of analytic structure in energy variables of the production amplitude.

1. INTRODUCTION

RECENTLY, Chan, Kajantie, and Ranft¹ have shown that a double-Regge-pole hypothesis suggested by Kibble² and by Ter-Martirosyan³ can be used to provide a reasonable fit to the data for such processes as $\pi^+p \rightarrow \pi^+\pi^0p$. Bali, Chew, and Pignotti^{4,5} have shown that an extension of Toller's work⁶ provides a plausible basis for generalizing the multi-Regge-pole hypothesis to arbitrary production amplitudes. The asymptotic form for production amplitudes that emerges from this work appears to be consistent with calculations of Polkinghorne⁷ based on perturbation theory and with the results of Gribov's Reggeon calculus.^{8,9}

In the case of two-body scattering, it is well known that the asymptotic behavior of the amplitude is influenced not only by Regge poles [Fig. 1(a)] but also by Regge cuts resulting from the exchange of two or more Regge poles [Fig. 1(b)]. Similar remarks apply to production amplitudes. The simplest multi-Regge-pole contribution to the process

$$1+2 \rightarrow 3+4+5$$

corresponds to Fig. 2(a) and the most straightforward types of correction are shown in Fig. 2(b). In addition, however, these are effects associated with the Reggeon

triangle graph of Fig. 3 and with similar, more complicated graphs

In Sec. 2, straightforward multi-Reggeon exchange is examined, using Gribov's⁸ approach. Some of the properties of the amplitude for coupling two Reggeons and a particle are examined in Sec. 3. Gribov's approach is applied also to the triangle graph in Sec. 4, and the resulting analytic structure and asymptotic behavior are considered in Secs. 5 and 6

Of course, the observability of effects due to the Reggeon triangle graph depends on the strength of the singularities with which they are associated. At present, just as in the two-body case, these are unknown. However, these effects have no analog in two-body scattering, so that their observation would be a striking encouragement for the relevance of a Reggeon calculus along the lines proposed by Gribov.⁸

2. DOUBLE-REGGE-POLE GRAPH

The double-Regge-pole graph [Fig. 2(a)] has presumably already been considered, using Gribov's techniques, in a paper by Anselm and Dyatlov (Ref. 3 of our Ref. 9). However, the work is not yet available, so that for completeness and to establish notation the problem will be reconsidered here. The Feynman amplitude, the asymptotic behavior of which is given by the double-Regge-pole graph, is shown in Fig. 4.

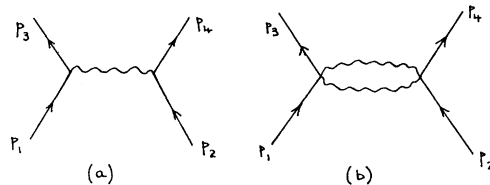


FIG. 1. (a) Regge-pole exchange; (b) two-Regge exchange giving rise to cuts.

¹ Chan Hong-Mo, K. Kajantie, and G. Ranft, *Nuovo Cimento* **49A**, 157 (1967); Chan Hong-Mo, K. Kajantie, G. Ranft, W. Beusch, and E. Flaminio, *ibid.* **51A**, 696 (1967).

² T. W. B. Kibble, *Phys. Rev.* **131**, 2282 (1963).

³ K. A. Ter-Martirosyan, *Nucl. Phys.* **68**, 591 (1965).

⁴ N. F. Bali, Geoffrey F. Chew, and Alberto Pignotti, *Phys. Rev.* **163**, 1572 (1967).

⁵ A set of references for various approaches to this problem is given in Ref. 4.

⁶ M. Toller, *Nuovo Cimento* **37**, 731 (1965).

⁷ J. C. Polkinghorne, *Nuovo Cimento* **36**, 857 (1965).

⁸ V. N. Gribov, *Zh. Exprim. i Teor. Fiz.* **53**, 654 (1967) [English transl.: *Soviet Phys.—JETP* **26**, 414 (1968)].

⁹ A. A. Anselm and I. T. Dyatlov, *Phys. Letters* **26B**, 100 (1967).

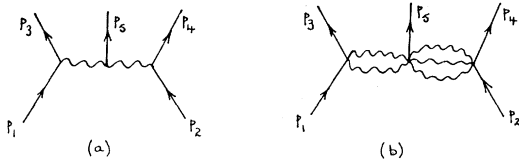


FIG. 2. (a) Double Regge-pole exchange; (b) multi-Reggeon exchange in a production amplitude.

The blobs A_1 and A_2 correspond to complete off-shell scattering amplitudes.

It is convenient to define the following momenta and invariants:

$$\begin{aligned} q_1 &= p_1 - p_3, & q_2 &= p_4 - p_2, \\ s &= (p_1 + p_2)^2 = (p_3 + p_4 + p_5)^2, & (1) \\ s_{35} &= (p_3 + p_5)^2, & s_{45} &= (p_4 + p_5)^2, \end{aligned}$$

so that q_1^2 and q_2^2 are the momentum transfers to be held fixed while the energy variables s , s_{35} , and s_{45} become infinite.

In the manner of Gribov⁸ it is assumed that the most singular behavior of the scattering amplitude A_1 occurs when q_1^2 and the scattering masses k^2 and $(k+q_1)^2$ remain finite and the "energy" $2p_1 \cdot k$ becomes infinite. The Regge hypothesis then implies that the important part of A_1 can be represented for large positive energy by

$$A_1 = g_1(q_1^2)G_1(q_1^2, 2p_1 \cdot k)g_1(q_1^2, k^2, (k+q_1)^2), \quad (2)$$

where

$$G_1 = -\frac{1}{4i} \int dj_1 \xi_{j_1} G_1(j_1, q_1^2) (2p_1 \cdot k)^{j_1}, \quad (3)$$

and the j_1 -integration contour lies entirely to the right of the singularities of $G_1(j_1, q_1^2)$. The signature factor is

$$\xi_{j_1} = (e^{-i\pi j_1} + \tau_1) / \sin \pi j_1, \quad (4)$$

where τ_1 is the signature. The large negative-energy limit is obtained by making the replacement

$$(2p_1 \cdot k)^{j_1} \rightarrow \tau_1 (-2p_1 \cdot k)^{j_1}$$

in Eq. (3). Simple Regge behavior comes from a pole at $j_1 = \alpha_1(q_1^2)$. Fully enhanced⁸ multi-Reggeon effects come from other singularities of G_1 . Similarly, the important part of A_2 can be written

$$A_2 = g_2(q_2^2)G_2(q_2^2, -2p_2 \cdot k)g_2(q_2^2, k^2, (k+q_2)^2), \quad (5)$$

where

$$G_2 = -\frac{1}{4i} \int dj_2 \xi_{j_2} G_2(j_2, q_2^2) (-2p_2 \cdot k)^{j_2}. \quad (6)$$

Assuming for convenience that the masses of all lines are equal to m^2 , the Feynman amplitude of Fig. 4 is given by

$$B(s, s_{35}, s_{45}, q_1^2, q_2^2) = -\frac{i}{(2\pi)^4} \int \frac{d^4k A_1 A_2}{(k^2 - m^2 + i\epsilon) [(k+q_1)^2 - m^2 + i\epsilon] [(k+q_2)^2 - m^2 + i\epsilon]}. \quad (7)$$

In order to investigate the behavior of B for large values of the energy variables, it is convenient to follow the Sudakov¹⁰ method, as suggested by Gribov,⁸ and define momenta

$$\begin{aligned} p_1' &= p_1 - (m^2/s)p_2, \\ p_2' &= p_2 - (m^2/s)p_1, \end{aligned} \quad (8)$$

such that $p_1'^2 \rightarrow p_2'^2 \rightarrow 0$ as $s \rightarrow \infty$. The loop momentum k may be resolved into components in the plane of p_1 and p_2 and perpendicular to it. That is,

$$k = \alpha p_2' + \beta p_1' + k', \quad (9)$$

where k' is a two-component spacelike vector perpendicular to p_1 and p_2 . For large s ,

$$d^4k = \frac{1}{2} |s| d\alpha d\beta d^2k'. \quad (10)$$

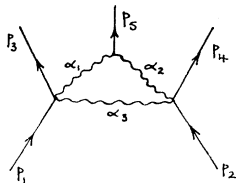


FIG. 3. Reggeon triangle graph.

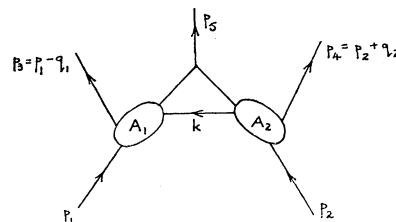


FIG. 4. Feynman diagram giving rise to double Regge-pole exchange.

¹⁰ V. V. Sudakov, Zh. Eksperim. i Teor. Fiz. **30**, 87 (1956) [English transl.: Soviet Phys.—JETP **3**, 65 (1956)].

where

$$\eta = M^2 - (q_1' - q_2')^2, \tag{14}$$

and consequently that, in this limit,

$$q_1'^2 = q_1'^2, \quad q_2'^2 = q_2'^2. \tag{15}$$

It follows that when s_{35} and s_{45} are large, so is s , and therefore

$$2k \cdot p_1 \cong \alpha s, \quad 2k \cdot p_2 \cong \beta s,$$

$$k^2 \cong \alpha \beta s + k'^2,$$

$$\begin{aligned} (k + q_1)^2 &\cong \alpha \beta s + \alpha s_{45} + (k' + q_1')^2, \\ (k + q_2)^2 &\cong \alpha \beta s - \beta s_{35} + (k' + q_2')^2. \end{aligned} \tag{16}$$

On substituting these relations into Eq. (7) together with the asymptotic form for A_1 and A_2 [Eqs. (2) and (5)], the leading contribution to the production amplitude is found to be

$$B = \left(-\frac{1}{4i} \right)^2 g_1(q_1'^2) g_2(q_2'^2) \int d j_1 d j_2 \xi_{j_1} \xi_{j_2} G_1(j_1, q_1'^2) G_2(j_2, q_2'^2) B_{j_1 j_2}(q_1', q_2', s_{35}, s_{45}), \tag{17}$$

where

$$\begin{aligned} B_{j_1 j_2} = & -\frac{i s}{2(2\pi)^4} \int d\alpha d\beta d^2 k' g_1(q_1'^2, k^2, (k + q_1)^2) g_2(q_2'^2, k^2, (k + q_2)^2) \\ & \times \frac{|\alpha s|^{j_1} |\beta s|^{j_2} [\theta(\alpha s) \pm \theta(-\alpha s)] [\theta(-\beta s) \pm \theta(\beta s)]}{(\alpha \beta s + k'^2 - m^2) [\alpha \beta s + \alpha s_{45} + (k' + q_1')^2 - m^2] [\alpha \beta s - \beta s_{35} + (k' + q_2')^2 - m^2]}, \end{aligned} \tag{18}$$

the \pm signs being determined by the signatures of the trajectories. Putting

$$\alpha s_{45} = \eta^{1/2} x, \quad \beta s_{35} = \eta^{1/2} y, \tag{19}$$

it follows that for positive s_{35}, s_{45} ,

$$B_{j_1 j_2} = s_{35}^{j_1} s_{45}^{j_2} f_{j_1 j_2}(q_1', q_2'), \tag{20}$$

where

$$f_{j_1 j_2} = \frac{-i}{2(2\pi)^4} \eta^{-\frac{1}{2}(j_1 + j_2)} \int d x d y d^2 k' g_1 g_2 \frac{|x|^{j_1} |y|^{j_2} [\theta(x) \pm \theta(-x)] [\theta(-y) \pm \theta(y)]}{(x y + k'^2 - m^2) [x y + \eta^{1/2} x + (k' + q_1')^2 - m^2] [x y - \eta^{1/2} y + (k' + q_2')^2 - m^2]}. \tag{21}$$

The asymptotic behavior of B is then

$$\begin{aligned} B = & g_1 g_2 \left(-\frac{1}{4i} \right)^2 \int d j_1 d j_2 s_{35}^{j_1} s_{45}^{j_2} \xi_{j_1} \xi_{j_2} \\ & \times G_1(j_1, q_1'^2) G_2(j_2, q_2'^2) f_{j_1 j_2}(q_1', q_2'). \end{aligned} \tag{22}$$

The limit for large negative s_{35} is obtained by making the replacement

$$s_{35}^{j_1} \rightarrow \tau_1 (-s_{35})^{j_1},$$

and similarly for large negative s_{45} .

When G_1 and G_2 have, as their right-most singularities, poles at $j_1 = \alpha_1(q_1'^2)$ and $j_2 = \alpha_2(q_2'^2)$, then the leading asymptotic behavior is

$$B \sim g_1 g_2 s_{35}^{\alpha_1} s_{45}^{\alpha_2} f_{\alpha_1 \alpha_2}(q_1'^2, q_2'^2, (q_1' - q_2')^2). \tag{23}$$

This result agrees with the conclusion of those authors mentioned in the Introduction. In particular, as emphasized in Refs. 1-4, $f_{\alpha_1 \alpha_2}$ depends not only on $t_1 = q_1'^2$ and $t_2 = q_2'^2$, but also on $q_3'^2 = (q_1' - q_2')^2$. In Ref. 1, this latter dependence is reduced to one on an azimuthal angle in the rest frame of particle 5.¹¹ It is also possible to interpret this dependence as one on the

¹¹ See Eq. (15) of Ref. 1. In this paper, particles 4 and 5 are interchanged relative to the conventions of this reference.

angle Ψ , between the production planes of particles 3 and 4 in either the lab or c.m. frame. That is,

$$\cos \Psi = q_1' \cdot q_2' / (t_1 t_2)^{1/2}. \tag{24}$$

This follows because, of course, $-q_1'$ and q_2' are the components of p_3 and p_4 transverse to the incident beam.

The dependence of the production amplitude on this variable is considered in more detail in Sec. 3.

Finally, note that Eq. (22) and related equations for negative values of s_{35} and s_{45} imply that asymptotically the analytic structure of B is simply the product of the s_{35} - and s_{45} -complex planes cut along their real axes. Of course, complicated structure and overlapping cuts may still exist at finite values of s_{35} and s_{45} . This property of asymptotic simplicity of analytic structure exists for more complicated diagrams and is essential in permitting the definition of an approximate double partial-wave amplitude in these cases.

3. BEHAVIOR OF THE TWO-REGGEON PARTICLE COUPLING

The dependence of $f_{\alpha_1 \alpha_2}$ on $q_3'^2$ may be crudely estimated by examining the singularity structure at $\eta = 0$. In order to do so, it is convenient to write Eq. (21)

in the form

$$f_{\alpha_1\alpha_2} = \eta^{-\frac{1}{2}(\alpha_1+\alpha_2)} \int dx dy |x|^{\alpha_1} |y|^{\alpha_2} [\theta(x) \pm \theta(-x)] [\theta(-y) \pm \theta(y)] F(xy, xy + \eta^{1/2}x, xy - \eta^{1/2}y), \tag{25}$$

where

$$F(w,u,v) = \frac{-i}{(2\pi)^4} \int \frac{d^2k' g_1(q_1'^2, w+k'^2, u+(k'+q_1')^2) g_2(q_2'^2, w+k'^2, v+(k'+q_2')^2)}{(w+k'^2-m^2+i\epsilon)[u+(k'+q_1')^2-m^2+i\epsilon][v+(k'+q_2')^2-m^2+i\epsilon]}. \tag{26}$$

If reasonable assumptions are made about g_1 and g_2 , namely, that they are analytic in the planes of their variables cut along the positive real axes, then $F(w,u,v)$ is analytic in the u, v , and w planes cut along the real axes from m^2 to infinity.

Equation (25) can be written

$$f_{\alpha_1\alpha_2} = \eta^{-\frac{1}{2}(\alpha_1+\alpha_2)} \int_0^\infty dx \int_0^\infty dy x^{\alpha_1} y^{\alpha_2} \times [F(-xy, -xy + \eta^{1/2}x, -xy + \eta^{1/2}y) + \tau_1 F(xy, xy - \eta^{1/2}x, xy + \eta^{1/2}y) + \tau_2 F(xy, xy + \eta^{1/2}x, xy - \eta^{1/2}y) + \tau_1\tau_2 F(-xy, -xy - \eta^{1/2}x, -xy - \eta^{1/2}y)]. \tag{27}$$

The last contribution to the integrand is the simplest one, since its singularities do not enter the integration region. The second contribution can be put in the same form by noting that for fixed (real) x the analyticity assumptions made above, together with the $i\epsilon$ prescription, permit the y -integration contour to be rotated anticlockwise through 180° . A similar analysis applied to the third contribution shows that for fixed (real) y the x -integration contour may be rotated. The distribution of singularities does not, however, permit the first term to be treated in this way. The result (assuming

that the contributions from infinity are zero) is

$$f_{\alpha_1\alpha_2} = \eta^{-\frac{1}{2}(\alpha_1+\alpha_2)} \int_0^\infty dx \int_0^\infty dy x^{\alpha_1} y^{\alpha_2} \times [F(-xy, -xy + \eta^{1/2}x, -xy + \eta^{1/2}y) + (\tau_1\tau_2 - e^{i\pi\alpha_1}\tau_2 - e^{i\pi\alpha_2}\tau_1) \times F(-xy, -xy - \eta^{1/2}x, -xy - \eta^{1/2}y)]. \tag{28}$$

As indicated above, the first contribution to the right side of Eq. (28) is the more complicated and will be discussed in detail. The second may be dealt with in an analogous fashion, and only the results are given below.

The motion of the singularities of the integrand in Eq. (28) makes it difficult to analyze the behavior of $f_{\alpha_1\alpha_2}$ as $\eta \rightarrow 0$. It is convenient, therefore, to change to integration variables that render this motion unimportant. For the first contribution in Eq. (28), convenient variables are

$$\begin{aligned} u &= xy - \eta^{1/2}x, \\ v &= xy - \eta^{1/2}y. \end{aligned} \tag{29}$$

It follows that

$$\begin{aligned} w &= xy = \frac{1}{2}(u+v + \eta \pm \sqrt{K}), \\ x &= \frac{1}{2}(v-u + \eta \pm \sqrt{K})/\eta^{1/2}, \\ y &= \frac{1}{2}(u-v + \eta \pm \sqrt{K})/\eta^{1/2}, \end{aligned} \tag{30}$$

where

$$K = K(u,v,\eta) = (u+v+\eta)^2 - 4uv, \tag{31}$$

and $K=0$ yields the parabola P , shown in Fig. 5, which touches the u and v axes at $(0, -\eta)$ and $(-\eta, 0)$. The Jacobian of the transformation is

$$J = \partial(u,v)/\partial(x,y) = \sqrt{K}. \tag{32}$$

The singular curves are

$$\begin{aligned} u &= -m^2, \\ v &= -m^2, \end{aligned} \tag{33}$$

and

$$w = -m^2,$$

that is,

$$(u+m^2)(v+m^2) + \eta m^2 = 0. \tag{34}$$

These curves are shown in Fig. 5. The attached cuts lie in the negative u and v directions.

When the $+$ sign is chosen in Eq. (30), the integration comprises the three quadrants in which either u or v is positive, together with the hatched region shown in

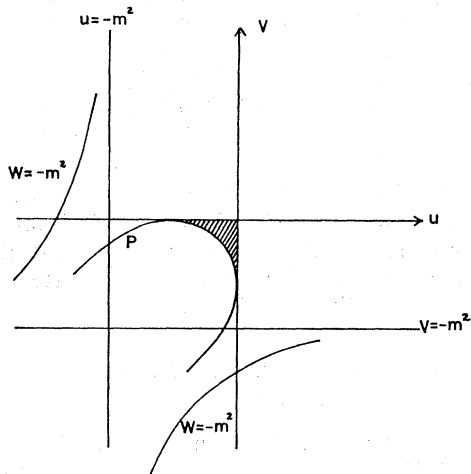


FIG. 5. Integration region and singularities in the (u,v) plane.

Fig. 5. When the $-$ sign is chosen, the integration region comprises only this hatched area.

As $\eta \rightarrow 0$, the only motion of the singular curves is that of the hyperbola [Eq. (34)] which coincides with its asymptotes [Eqs. (33)]. The $i\epsilon$ prescription guarantees that no pinch of the integration contour occurs. It follows that the relationship of the singular curves to the integration contour does not change significantly as $\eta \rightarrow 0$.

The contribution from the hatched area can be most simply estimated by noting that it corresponds to the

box $0 \leq x \leq \eta^{1/2}$, $0 \leq y \leq \eta^{1/2}$ in the (x, y) plane. Hence, for small η this contribution is given by

$$\eta^{-\frac{1}{2}(\alpha_1 + \alpha_2)} F(0, 0, 0) \int_0^{\eta^{1/2}} dx x^{\alpha_1} \int_0^{\eta^{1/2}} dy y^{\alpha_2} = \frac{\eta F(0, 0, 0)}{(1 + \alpha_1)(1 + \alpha_2)}. \quad (35)$$

The singular contribution to $f_{\alpha_1 \alpha_2}$ coming from the first term in Eq. (28) is therefore

$$f_{\alpha_1 \alpha_2}^{(1)} = \eta^{-(\alpha_1 + \alpha_2)} \int \frac{dudv}{[K(u, v, \eta)]^{1/2}} \left[\frac{1}{2}(v - u + \eta + \sqrt{K}) \right]^{\alpha_1} \left[\frac{1}{2}(u - v + \eta + \sqrt{K}) \right]^{\alpha_2} F(-w, -u, -v), \quad (36)$$

the integration region being the above-mentioned three quadrants. Equation (36) may be written

$$\begin{aligned} f_{\alpha_1 \alpha_2}^{(1)} &= \eta^{-\alpha_2} \int_{u \geq v} \frac{dudv}{\sqrt{K}} \left[\frac{1}{2}(u + v + \eta + \sqrt{K}) \right]^{\alpha_1} \\ &\quad \times \left[\frac{1}{2}(u - v + \eta + \sqrt{K}) \right]^{\alpha_2 - \alpha_1} F(-w, -u, -v) \\ &+ \eta^{-\alpha_1} \int_{v \geq u} \frac{dudv}{\sqrt{K}} \left[\frac{1}{2}(u + v + \eta + \sqrt{K}) \right]^{\alpha_2} \\ &\quad \times \left[\frac{1}{2}(v - u + \eta + \sqrt{K}) \right]^{\alpha_1 - \alpha_2} F(-w, -u, -v). \end{aligned} \quad (37)$$

This equation does not yield the behavior of $f_{\alpha_1 \alpha_2}$ immediately, since, when $\alpha_1 \geq \alpha_2$, the first integral diverges as $\eta \rightarrow 0$ because of a singularity on the line $u = v$. When $\alpha_2 \geq \alpha_1$, the second integral diverges. The difficulty can be overcome, however, by dividing each integration region thus:

$$\begin{aligned} u \geq v &\rightarrow u \geq v + c, \quad v + c \geq u \geq v; \\ v \geq u &\rightarrow v \geq u + c, \quad u + c \geq v \geq u. \end{aligned}$$

For small η , Eq. (37) becomes

$$\begin{aligned} f_{\alpha_1 \alpha_2}^{(1)} &= \eta^{-\alpha_2} \int_{u \geq v+c} dudv u^{\alpha_1} (u-v)^{\alpha_2 - \alpha_1 - 1} F(-w, -u, -v) + \eta^{-\alpha_1} \int_{v \geq u+c} dudv v^{\alpha_2} (v-u)^{\alpha_1 - \alpha_2 - 1} F(-w, -u, -v) \\ &+ \eta^{-\alpha_2} \int_0^\infty du u^{\alpha_1} \int_\eta^{c+\eta} \frac{dz}{(z^2 + 4u\eta)^{1/2}} \left\{ \frac{1}{2}[z + (z^2 + 4u\eta)^{1/2}] \right\}^{\alpha_2 - \alpha_1} F(-u, -u, -u) \\ &+ \eta^{-\alpha_1} \int_0^\infty dv v^{\alpha_2} \int_\eta^{c+\eta} \frac{dz}{(z^2 + 4v\eta)^{1/2}} \left\{ \frac{1}{2}[z + (z^2 + 4v\eta)^{1/2}] \right\}^{\alpha_1 - \alpha_2} F(-v, -v, -v), \end{aligned} \quad (38)$$

where the substitution $z = (v - u + \eta)$ or $(u - v + \eta)$ is made as appropriate, and c is chosen sufficiently small that $u = v$ is a good approximation in the third and fourth terms. In addition, η has been taken equal to zero where this does not cause trouble. Of course, the convergence of the resulting integrals at infinity is a further assumption.

The z integrations can be performed explicitly. For example,

$$\begin{aligned} \int_\eta^{c+\eta} \frac{dz}{(z^2 + 4u\eta)^{1/2}} \left\{ \frac{1}{2}[z + (z^2 + 4u\eta)^{1/2}] \right\}^{\alpha_2 - \alpha_1} \\ = (\alpha_2 - \alpha_1)^{-1} [c^{\alpha_2 - \alpha_1} - (u\eta)^{\frac{1}{2}(\alpha_2 - \alpha_1)}]. \end{aligned} \quad (39)$$

It then follows that as $\eta \rightarrow 0$,

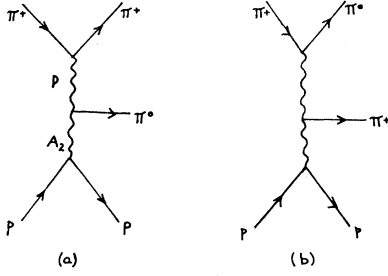
$$f_{\alpha_1 \alpha_2}^{(1)} \cong A_1 \eta^{-\alpha_1} + A_2 \eta^{-\alpha_2}, \quad (40)$$

where

$$\begin{aligned} A_1 &= \int_{u \geq v+c} dudv u^{\alpha_2} (v-u)^{\alpha_1 - \alpha_2 - 1} F(-w, -u, -v) \\ &\quad + \frac{c^{(\alpha_1 - \alpha_2)}}{\alpha_1 - \alpha_2} \int_0^\infty dv v^{\alpha_2} F(-v, -v, -v), \end{aligned} \quad (41)$$

$$\begin{aligned} A_2 &= \int_{u \geq v+c} dudv u^{\alpha_1} (u-v)^{\alpha_2 - \alpha_1 - 1} F(-w, -u, -v) \\ &\quad + \frac{c^{(\alpha_2 - \alpha_1)}}{\alpha_2 - \alpha_1} \int_0^\infty du u^{\alpha_1} F(-u, -u, -u). \end{aligned}$$

The term in $\eta^{-\frac{1}{2}(\alpha_1 + \alpha_2)}$ from the third contribution in Eq. (38) is cancelled by a similar term in the fourth contribution. Note that A_1 and A_2 both have a pole at

FIG. 6. Reggeon graphs for the process $\pi^+ p \rightarrow \pi^+ \pi^0 p$.

$\alpha_1 = \alpha_2$ but the residues are opposite. When $\alpha_1 = \alpha_2$, the behavior is changed slightly to become

$$f_{\alpha_1 \alpha_2}^{(1)} \cong \eta^{-\alpha} (A - B \ln \eta). \quad (42)$$

The second term on the right of Eq. (28) yields behavior of the same form and thus contributes simply to a modification of the coefficients A_1 and A_2 in Eq. (40). The behavior indicated in Eq. (40) agrees with that suggested by Blankenbecler and Sugar.¹² Both Eqs. (40) and (42) confirm the results of Zakrzewski,¹³ who has examined the two-Reggeon graph in perturbation theory. Strictly speaking, the analysis set out above is relevant to the variation of $f_{\alpha_1 \alpha_2}$ with η when $q_3'^2$ is fixed. In other words, the analysis really yields the dependence of $f_{\alpha_1 \alpha_2}$ on M^2 . However, when M^2 is fixed and $q_3'^2$ is allowed to vary, one would, in general, expect the same results to hold unless there is an accidental relation between M and the internal masses. If it is assumed that A_1 and A_2 (or A and B) do not vary rapidly with $q_3'^2$, then Eqs. (40) and (42) provide an estimate for the dependence of $f_{\alpha_1 \alpha_2}$ on η .

It would be of interest to test Eqs. (40) and (42) experimentally. In order to do so, it is necessary that variations in Ψ produce appreciable changes in η . This requires M^2 to be small ($M^2 \lesssim |t_1|, |t_2|$), the most favorable case being $M^2 = m_\pi^2$. An interesting process to consider is $\pi^+ p \rightarrow \pi^+ \pi^0 p$. The most clear-cut situation

arises when¹ π^0 is chosen as particle 5, since then there is a single important two-Reggeon contribution comprising the Pomeranchuk and A_2 trajectories [Fig. 6(a)]. When $|t_1| = |t_2| = 0.25 \text{ BeV}^2$, then the physical range for η is $0.02 \leq \eta \leq 1 \text{ BeV}^2$. If the estimates $\alpha_P = 1.0$ and $\alpha_{A_2} = 0.5$ are accepted, then Eq. (40) predicts that $f_{\alpha_P \alpha_{A_2}}$ has one term that increases by a factor of 50 and another that increases by a factor of 7 as η is reduced through its physical range.

If π^+ is chosen as particle 5, then there are two important contributions, shown in Fig. 6(b). In this case, the estimates $\alpha_p \cong \alpha_\omega \cong \alpha_{A_2} \cong 0.5$ lead to a variation of the amplitude by a factor of 7 as η is reduced through its physical range.

Unfortunately, the small mass of the pion, which is essential to the striking character of the above variations, also makes an examination of the entire physical range for η out of the question at present energies. In order that the entire range lie in the asymptotic region, it is necessary that $m_\pi^2 s \geq s_0^2$, where s_0 represents the lower end of the asymptotic region for the subenergies S_{35} and S_{45} . This implies that the lab energy of the pion, w , must satisfy $w \geq s_0^2 / 2m_\pi^2 m_N$. If $s_0 \cong 10 \text{ BeV}^2$ (a rather low value), then $w \cong 2.5 \times 10^8 \text{ BeV}$. However, it would still be possible to examine values of $\eta > 0.5 \text{ BeV}^2$ with a pion lab energy of 100 BeV. A variation by a factor of 2 of the amplitude associated with Fig. 6(a) in the range $0.5 \leq \eta \leq 1.0 \text{ BeV}^2$ would be expected on the above reasoning

4. REGGEON TRIANGLE GRAPH

The Reggeon triangle graph of Fig. 3 determines the asymptotic behavior of the Feynman amplitude illustrated in Fig. 7. That part of the diagram enclosed in the dashed boundary is just the off-shell-mass version of the amplitude B considered in Sec. 2. The Feynman amplitude is therefore given by (the momenta are indicated in Fig. 7)

$$T = - \left(\frac{i}{(2\pi)^4} \right)^3 \int \frac{d^4 k d^4 k_1 d^4 k_2 B A_3}{(k_1^2 - m^2)[(p_1 - k_1)^2 - m^2][(k_1 - k)^2 - m^2][(p_1 - k_1 - q_1 + k)^2 - m^2]} \times \{ (k_2^2 - m^2)[(p_2 - k_2)^2 - m^2][(k_2 + k)^2 - m^2][(p_2 + q_2 - k_2 - k)^2 - m^2] \}^{-1}. \quad (43)$$

Once again, it is convenient to introduce the Sudakov variables

$$k_i = \alpha_i p_2' + \beta_i p_1' + k_i', \quad (44)$$

so that, for large s ,

$$d^4 k_i = \frac{1}{2} |s| d\alpha_i d\beta_i d^2 k_i'. \quad (45)$$

The invariant quantities entering into the loop at the

¹² R. Blankenbecler and R. L. Sugar, Phys. Rev. **168**, 1597 (1968).

¹³ I would like to thank Dr. J. C. Polkinghorne and W. J. Zakrzewski for discussions on this point. The work of Zakrzewski will appear soon as a Cambridge University Report.

left end of Fig. 7 are, for large s , s_{35} , and s_{45} ,

$$\begin{aligned} k_1^2 &= \alpha_1 \beta_1 s + k_1'^2, \\ (p_1 - k_1)^2 &= \alpha_1 \beta_1 s - \alpha_1 s + m^2 (1 - \beta_1) + k_1'^2, \\ (k - k_1)^2 &= (\alpha - \alpha_1)(\beta - \beta_1) s + (k' - k_1')^2, \\ (p_1 - k_1 + k - q_1)^2 &= (\alpha - \alpha_1)(\beta - \beta_1) s \\ &\quad + (1 - s_{45}/s)(\alpha - \alpha_1) s \\ &\quad + (1 + \beta - \beta_1 - s_{45}/s) m^2 \\ &\quad + (k_1' - k' + q_1')^2. \end{aligned} \quad (46)$$

It will also be assumed here that the most singular

behavior of the integrand arises when the internal masses such as those given in Eq. (46) remain finite and the internal energies $(k_1+k_2)^2$, $(p_3-k_1+k+p_5)^2$, and $(p_4-k_2-k+p_5)^2$ become infinite. It follows, from arguments entirely analogous to those used by Gribov⁸ in the two-body case, that any finite region of the invariants in Eq. (46) is such that

$$\begin{aligned} \alpha_1 &\sim m^2/s, & (\alpha-\alpha_1) &\sim m^2/s, \\ \beta &\sim 1, & (\beta-\beta_1) &\sim 1, \end{aligned} \tag{47}$$

for large s . Hence, if only the most singular contribution to the asymptotic behavior is sought, then in other parts of the diagram α_1 and α may be set equal to zero. A similar argument involving invariants in the twisted loop at the right of Fig. 7 shows that the leading asymptotic behavior is controlled by regions where

$$\begin{aligned} \beta_2 &\sim m^2/s, & (\beta-\beta_1) &\sim m^2/s, \\ \alpha_2 &\sim 1, & (\alpha-\alpha_2) &\sim 1. \end{aligned} \tag{48}$$

Hence, in other parts of the diagram β and β_2 may be set equal to zero. In these circumstances the asymptotic energy variables become, for large s ,

$$\begin{aligned} (k_1+k_2)^2 &= \alpha_2\beta_2s, \\ (p_3-k_1-k+p_5)^2 &= (1-\beta)s_{35}, \\ (p_4-k_2-k+p_5)^2 &= (1-\alpha_2)s_{45}. \end{aligned} \tag{49}$$

The important contribution from A_3 may then be written

$$\begin{aligned} A_3 &= g_3(k^2, k_1^2, (k-k_1)^2)G_3(k^2(k_1+k_2)^2) \\ &\quad \times g_3(k^2, k_2^2, (k+k_2)^2), \\ G_3 &= -\frac{1}{4i} \int dl_3 \xi_{l_3} G_3(l_3, k^2) (\alpha_2\beta_1s)^{l_3}, \end{aligned} \tag{50}$$

and that from B may be written

$$\begin{aligned} B &= \left(-\frac{1}{4i}\right)^2 g_1 g_2 \int dl_1 dl_2 \xi_{l_1} \xi_{l_2} \\ &\quad \times (1-\beta_1)^{l_1} (1-\alpha_2)^{l_2} s_{35}^{l_1} s_{45}^{l_2} \\ &\quad \times G_1(l_1, (q_1'-k')^2) G_2(l_2, (q_2'-k')^2) \\ &\quad \times f_{l_1 l_2}(q_1'-k', q_2'-k'). \end{aligned} \tag{51}$$

When these expressions are inserted into Eq. (43), the result is

$$\begin{aligned} T &= \frac{i\pi}{2|s_{35}|} \frac{i\pi}{2|s_{45}|} \int \frac{d^2k'}{(2\pi)^2} \frac{dl_1 dl_2 dl_3}{(2\pi i)^3} \frac{i}{\xi_{l_3} \eta^{l_3-1}} \\ &\quad \times N_{l_1 l_3}(q_1', k') N_{l_2 l_3}(q_2', k') G_1 G_2 G_3 f_{l_1 l_2}(q_1'-k', q_2'-k') \\ &\quad \times \xi_{l_1} \xi_{l_3} (s_{35})^{l_1+l_3} \xi_{l_2} \xi_{l_3} (s_{45})^{l_2+l_3}, \end{aligned} \tag{52}$$

where $N_{l_1 l_3}(q_1', k')$ is the amplitude defined by Gribov⁸ corresponding to the graph of Fig. 8.

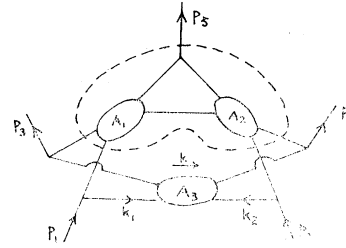


FIG. 7. Feynman diagram corresponding to the Reggeon triangle graph.

It is easy to check that T is even or odd in s_{35} according as the signatures of trajectories 1 and 3 are equal or opposite. In fact, Eq. (52) can be regarded as yielding the asymptotic behavior of s_{35} in the upper half s_{35} plane, while that in the lower half-plane is obtained by replacing $s_{35}^{l_1+l_3-1}$ with $\tau_1 \tau_3 (-s_{35})^{l_1+l_3-1}$. Once again, it is implicit in the analysis that asymptotically the production amplitude enjoys simple cut-plane analyticity in s_{35} and, of course, in s_{45} as well. With these considerations in mind, it is easy to check that for large positive s_{35} the asymptotic absorptive part is obtained from Eq. (52) by replacing $i\xi_{l_1} \xi_{l_3}$ with $\gamma_{l_1 l_3}$, where

$$\gamma_{l_1 l_3} = \frac{1}{2} \xi_{l_1} \xi_{l_3} (1 + \tau_1 \tau_3 e^{i\pi(l_1+l_3)}). \tag{53}$$

(In fact, $\gamma_{l_1 l_3} = \text{Re} \xi_{l_1} \xi_{l_3}$ when l_1 and l_3 are real.) A similar discussion yields the s_{45} absorptive part. The double absorptive part is then

$$\begin{aligned} t &= i \left(\frac{1}{2}\pi\right)^2 \int \frac{d^2k'}{(2\pi)^2} \frac{dl_1 dl_2 dl_3}{(2\pi i)^3} \gamma_{l_1 l_3} \gamma_{l_2 l_3} \\ &\quad \times N_{l_1 l_3} N_{l_2 l_3} G_1 G_2 G_3 f_{l_1 l_2} s_{35}^{l_1+l_3-1} s_{45}^{l_2+l_3-1}. \end{aligned} \tag{54}$$

The “double partial-wave” amplitude, insofar as its right-most singularities are concerned, may be calculated as

$$T_{j_1 j_2} = \left(\frac{2}{\pi}\right)^2 \int_{s_A} ds_{35} s_{35}^{-j_1-1} \int_{s_A} ds_{45} s_{45}^{-j_2-1} t, \tag{55}$$

where s_A is some arbitrary lower limit. The result, keeping only singularities furthest to the right, is

$$\begin{aligned} T_{j_1 j_2} &= i \int \frac{d^2k'}{(2\pi)^2} \frac{dl_1 dl_2 dl_3}{(2\pi i)^3} \\ &\quad \times \frac{N_{l_1 l_3} N_{l_2 l_3} \gamma_{l_1 l_3} \gamma_{l_2 l_3} G_1 G_2 G_3 f_{l_1 l_2}}{\xi_{l_3} \eta^{l_3-1} (j_1-l_1-l_3+1)(j_2-l_2-l_3+1)}. \end{aligned} \tag{56}$$

If now only the pole contributions from the G_i are kept,

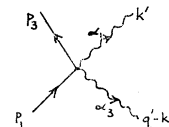


FIG. 8. Graph for coupling two Reggeons to two external particles.

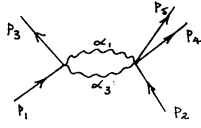


FIG. 9. Contraction of the Reggeon triangle graph.

the background terms being dropped, the result is

$$T_{j_1 j_2} = i \int \frac{d^2 k'}{(2\pi)^2} \frac{\gamma_{\alpha_1 \alpha_3} \gamma_{\alpha_2 \alpha_3}}{\xi_{\alpha_3} \eta^{\alpha_3 - 1}} \times \frac{N_{\alpha_1 \alpha_3} N_{\alpha_2 \alpha_3} f_{\alpha_1 \alpha_2}}{(j_1 - \alpha_1 - \alpha_2 + 1)(j_2 - \alpha_1 - \alpha_3 + 1)}, \quad (57)$$

where, of course,

$$\begin{aligned} \alpha_1 &= \alpha_1((k' - q_1')^2), \\ \alpha_2 &= \alpha_2((k' - q_2')^2), \\ \alpha_3 &= \alpha_3(k'^2). \end{aligned} \quad (58)$$

Equation (57) suggests that Gribov's rules with suitable modifications will apply in calculating the Reggeon graphs for production amplitudes. The modifications are that for each three-Reggeon loop to which an external particle is attached, there must be (i) a factor $f_{l_1 l_2}$ for the coupling of Reggeons 1 and 2 to the external particle, (ii) a factor $\gamma_{l_2 l_3}$ for the "absorbing" vertex as well as $\gamma_{l_1 l_3}$ for the "emitting" vertex, and (iii) a factor $i(\xi_{l_3} \eta^{l_3 - 1})$ associated with the third Reggeon in the loop. One consequence of these changes is that the Reggeon "Ward identity" suggested by Anselm and Dyatlov⁹ no longer holds when the particle-two-Reggeon vertex is modified by a Reggeon insertion.

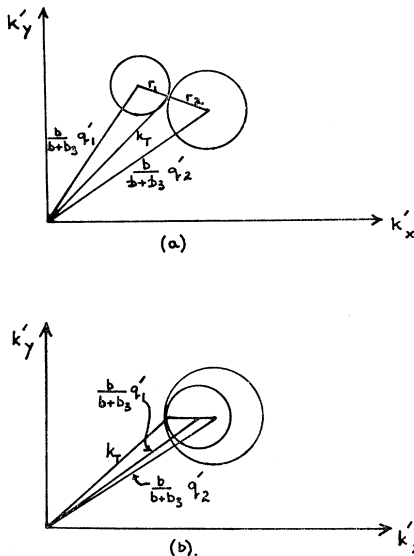


FIG. 10. Pinch giving rise to the leading singular curve of the triangle graph (a) in the limit $(j_1 \pm i\epsilon, j_2 \pm i\epsilon)$, (b) in the limit $(j_1 \pm i\epsilon, j_2 \mp i\epsilon)$.

5. ANALYTIC STRUCTURE OF $T_{j_1 j_2}$

The complete analytic structure of $T_{j_1 j_2}$ cannot be understood without a knowledge of the properties of the numerator in Eq. (57). However, it is possible to give an account of that part which arises from pinches caused by the vanishing of the denominator.

To simplify the discussion, it will be supposed that the trajectories are linear, that is,

$$\alpha_i(t) = a_i + b_i t, \quad (59)$$

and that $a_1 = a_2 = a, b_1 = b_2 = b$. The zeros of the denominator are two circles in the k' plane, one with center

$$k' = [b/(b+b_3)]q_1' \quad (60)$$

and radius r_1 , where

$$r_1^2 = \frac{a+a_3-j_1-1}{b+b_3} + \frac{bb_3}{(b+b_3)^2} q_1'^2, \quad (61)$$

and the other with center

$$k' = [b/(b+b_3)]q_2' \quad (62)$$

and radius r_2 , where

$$r_2^2 = \frac{a+a_3-j_2-1}{b+b_3} + \frac{bb_3}{(b+b_3)^2} q_2'^2. \quad (63)$$

When j_1 and j_2 are sufficiently large, r_1^2 and r_2^2 are negative. The denominator never vanishes and the function is analytic in both variables. When j_1 is reduced so far that $r_1^2 = 0$, then the k' integration is pinched and a singularity of $T_{j_1 j_2}$ results at the point

$$j_1 = \alpha_{13}(q_1'^2) = a + a_3 + [bb_3/(b+b_3)]q_1'^2 - 1. \quad (64)$$

This is just the two-Reggeon cut corresponding to the contracted diagram in Fig. 9. Similarly, when j_2 attains the value

$$j_2 = \alpha_{23}(q_2'^2) = a + a_3 + [bb_3/(b+b_3)]q_2'^2 - 1, \quad (65)$$

r_2 vanishes and $T_{j_1 j_2}$ is again singular.

When $j_1 < \alpha_{13}, j_2 < \alpha_{23}$, so that r_1 and r_2 are real, then the leading singular curve, corresponding to the complete triangle diagram, is encountered. It results from a pinch occurring when the two circles touch (see Fig. 10), that is, when

$$(r_1 \pm r_2)^2 = -[b/(b+b_3)]^2 q_3'^2. \quad (66)$$

This curve is a parabola (see Fig. 11) that touches the line $j_1 = \alpha_{13}(q_1'^2)$ at

$$j_2 = \alpha_{23} + [bb_3/(b+b_3)]q_3'^2 \quad (67)$$

and the line $j_2 = \alpha_{23}$ at the symmetrical point.

In determining those parts where the leading curve is singular, it is necessary to take into account the cuts attached to the branch points given by Eqs. (64) and (65). Since the leading curve lies in a region through

which both cuts pass, it is necessary to specify the sign of the small imaginary parts ϵ_1 and ϵ_2 of j_1 and j_2 at points on the curve. When ϵ_1 and ϵ_2 have the same sign, the pinch that gives rise to the leading curve is effective¹⁴ when the circles touch as in Fig. 10(a). The corresponding part of the leading curve lies between its touching points with the two-Reggeon branch points. It turns out that this is the part of the curve that determines physical asymptotic behavior. The remainder of the curve corresponds to a pinch of the type shown in Fig. 10(b) and is singular when ϵ_1 and ϵ_2 have opposite signs.

The relationship between this analytic structure and asymptotic behavior is examined in Sec. 6. In order to make the connection, it is useful to understand the discontinuities of $T_{j_1 j_2}$ around its singularities.

The discontinuity around the branch point $j_1 = \alpha_{13}(q_1'^2)$ is obtained by replacing, in Eq. (57), the relevant pole with a δ function. The result is

$$\begin{aligned} \Delta_1 T_{j_1 j_2} &= 2\pi \int \frac{d^2 k'}{(2\pi)^2} \delta[j_1 - \alpha_1(k'^2) - \alpha_3((k' - q_1')^2) + 1] \\ &\quad \times \frac{\gamma_{\alpha_1 \alpha_3} \gamma_{\alpha_2 \alpha_3} N_{\alpha_1 \alpha_3} N_{\alpha_2 \alpha_3} f_{\alpha_1 \alpha_2}}{\xi_{\alpha_3} \eta^{\alpha_3 - 1} (j_2 - \alpha_2 - \alpha_3 + 1)}. \end{aligned} \quad (68)$$

The value of the discontinuity may be approximately evaluated near threshold by replacing k' with $[b/(b+b_3)]q_1'$ everywhere in the integrand except the δ function, with the result that

$$\Delta_1 T_{j_1 j_2} \cong \frac{\gamma_{\alpha_1 \alpha_3} \gamma_{\alpha_2 \alpha_3} N_{\alpha_1 \alpha_3} N_{\alpha_2 \alpha_3} f_{\alpha_1 \alpha_2}}{2(b+b_3)\xi_{\alpha_3} \eta^{\alpha_3 - 1} (j_2 - \alpha_2 - \alpha_3 + 1)}. \quad (69)$$

It follows that in this approximation, where $N_{\alpha_1 \alpha_3}$ does not depend on j_1 , the singularity $j_1 = \alpha_{13}(q_1'^2)$ is logarithmic. Although it is only approximate, Eq. (69) exhibits the important property that while it contains the leading singularity represented by a pole at

$$j_2 = \alpha_{23}(q_2'^2) + [bb_3/(b+b_3)]q_3'^2,$$

$\Delta_1 T_{j_1 j_2}$ does not contain the two-Reggeon cut beginning at $j_2 = \alpha_{23}(q_2'^2)$. This latter property is exact and follows from the presence of the δ function in Eq. (68) which restricts the k' integration to the circle

$$\{k' - [b/(b+b_3)]q_3'\}^2 + r_1^2 = 0.$$

In general, this restricted contour will not be pinched when $j_2 = \alpha_{23}(q_2'^2)$.

The discontinuity of $T_{j_1 j_2}$ across the cut attached to the leading curve is obtained by replacing both poles of

¹⁴ The relevant theory of pinching is explained in the appendix of P. V. Landshoff and D. I. Olive, *J. Math. Phys.* **7**, 1464 (1966), and also in M. J. Bloxham, D. I. Olive, and J. C. Polkinghorne, *ibid.* (to be published).

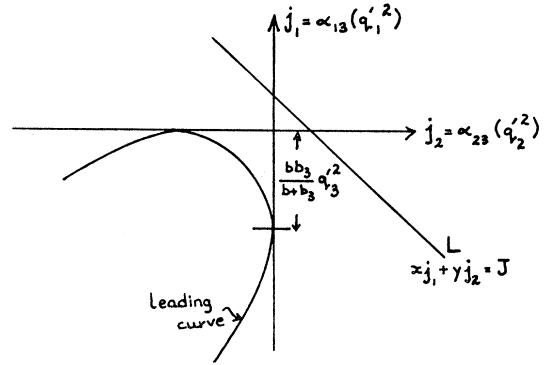


FIG. 11. Leading singular curve of the Reggeon triangle graph.

the integrand in Eq. (57) with δ functions. The result is

$$\begin{aligned} \Delta_{12} T_{j_1 j_2} &= -i \int d^2 k' \delta(j_1 - \alpha_1 - \alpha_3 + 1) \delta(j_2 - \alpha_2 - \alpha_3 + 1) \\ &\quad \times (\xi_{\alpha_3} \eta^{\alpha_3 - 1})^{-1} \gamma_{\alpha_1 \alpha_3} \gamma_{\alpha_2 \alpha_3} N_{\alpha_1 \alpha_3} N_{\alpha_2 \alpha_3} f_{\alpha_1 \alpha_2}. \end{aligned} \quad (70)$$

It can be evaluated approximately in the neighborhood of the singularity by replacing k' with its value k_T' at the touching point in Fig. 10, everywhere in the integrand except the δ functions. The conclusion is that near the singularity,

$$\begin{aligned} \Delta_{12} T_{j_1 j_2} &\{ (r_1 + r_2)^2 - [b/(b+b_3)]^2 q_3'^2 \}^{-1/2} \\ &\times \{ (r_1 - r_2)^2 - [b/(b+b_3)]^2 q_3'^2 \}^{-1/2}, \end{aligned} \quad (71)$$

so that the discontinuity has inverse-square-root behavior.

6. ASYMPTOTIC BEHAVIOR

The production amplitude is obtained from the double partial wave $T_{j_1 j_2}$ by writing

$$T(s, s_{35}, s_{45}, t_1, t_2) = \left(\frac{-1}{4i}\right)^2 \int d j_1 d j_2 \xi_{j_1} \xi_{j_2} T_{j_1 j_2} s_{35}^{j_1} s_{45}^{j_2}. \quad (72)$$

Since the analytic structure of $T_{j_1 j_2}$ is no longer a product of two factors, each with singularities in *one* variable, the asymptotic behavior of T no longer has a simple product form. A convenient way of understanding the asymptotic character of T is to introduce a limit suggested by Polkinghorne⁷ on the basis of a perturbation-theory investigation. Put

$$\begin{aligned} s_{35} &= \lambda(\eta s)^x, \\ s_{45} &= \lambda^{-1}(\eta s)^y, \end{aligned} \quad (73)$$

$$x + y = 1.$$

Then

$$s_{35}^{j_1} s_{45}^{j_2} = \lambda^{j_1 - j_2} (\eta s)^{x j_1 + y j_2}. \quad (74)$$

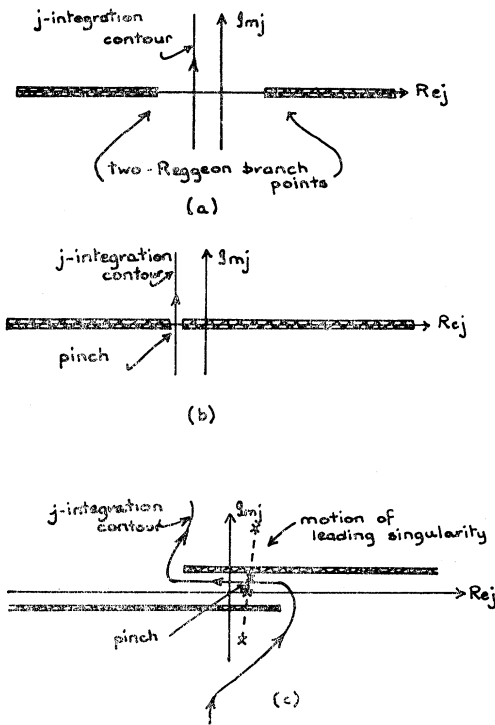


FIG. 12. (a) The j -integration contour. (b) Pinch of the j contour by the two-Reggeon singularities. (c) Pinch of the j contour by the leading curve singularities.

On making the change of variables

$$\begin{aligned} J &= xj_1 + yj_2, \\ j &= j_1 - j_2, \end{aligned} \tag{75}$$

Eq. (72) can be put in the form

$$T = -\frac{1}{4i} \int dJ \varphi(J) (s)^J, \tag{76}$$

where

$$\varphi(J) = -\frac{1}{4i} \int dj \xi_{j_1} \xi_{j_2} \lambda^j T_{j_1 j_2}, \tag{77}$$

with

$$\begin{aligned} j_1 &= J + yj, \\ j_2 &= J - xj. \end{aligned} \tag{78}$$

The J integration may be chosen to run from $-i\infty$ to $+i\infty$, with $\text{Re}J$ sufficiently large. In that case, the j interaction (at fixed J) runs between the singularities that correspond to the branch points $j_1 = \alpha_{13}(q_1'^2)$, $j_2 = \alpha_{23}(q_2'^2)$ as indicated in Fig. 12(a).

The s -asymptotic behavior of T is determined by the right-most singularity of $\varphi(J)$. Such singularities arise from pinches of the j -integration contour in Eq. (77). Since this contour lies in the complex part of the line L , shown in Fig. 11 and given by

$$xj_1 + yj_2 = J,$$

it is clear that pinches are brought about by (i) the

coincidence of the two-Reggeon branch points [Fig. 12(b)] when

$$J = x\alpha_{13}(q_1'^2) + y\alpha_{23}(q_2'^2) \tag{79}$$

and (ii) the leading curve when L becomes tangent to it [Fig. 12(c)].

Pinch (i) is ineffective and results in no singularity of $\varphi(J)$ because, as pointed out in Sec. 5, $\Delta_{12}T_{j_1 j_2}$ does not contain the singularity at $j_2 = \alpha_{23}(q_2'^2)$. It is easily verified that this property implies that no discontinuity of $\varphi(J)$ results from continuing around the point given in Eq. (79).

The right-most singularity of $\varphi(J)$ is, therefore, produced by pinch (ii). This occurs at the point

$$J = x\alpha_{13}(q_1'^2) + y\alpha_{23}(q_2'^2) + xy[b^2/(b+b_3)]q_3'^2, \tag{80}$$

when also

$$\begin{aligned} j_1 &= \alpha_{13}(q_1'^2) + y^2[b/(b+b_3)]q_3'^2, \\ j_2 &= \alpha_{23}(q_2'^2) + x^2[b/(b+b_3)]q_3'^2. \end{aligned} \tag{81}$$

It is simple to check that the inverse-square-root behavior of $\Delta_{12}T_{j_1 j_2}$ [Eq. (71)] implies that the discontinuity of $\varphi(J)$ is analytic at the branch point. The resulting asymptotic behavior is then

$$T \sim s^J / \ln s$$

at fixed $(q_1'^2, q_2'^2, q_3'^2)$, where J is given by Eq. (80). The behavior arising from the Reggeon triangle graph therefore differs from that due to a double Reggeon graph, in that the exponent of s depends on $q_3'^2$ as well as on $q_1'^2$ and $q_2'^2$. Associated with this extra dependence of the exponent is a nonlinear one on x and y , which determine the relative rates at which s_{35} and s_{45} become infinite.

CONCLUSION

In this paper, Gribov's approach has been used to investigate the asymptotic properties of production amplitudes. When it is applied to an analysis of the double-Reggeon-exchange graph, the results of previous authors are confirmed. In particular, it is verified that the amplitudes for the coupling of two Reggeons to an external particle $f_{\alpha_1 \alpha_2}$ depend not only on the masses of the Reggeons $q_1'^2$ and $q_2'^2$, but also on $q_3'^2 = (q_1' - q_2')^2$. On the basis of a Feynman-diagram model, the analytic properties of $f_{\alpha_1 \alpha_2}$ as a function of $q_3'^2$ are discussed. It is shown that when $\alpha_1 \neq \alpha_2$ and $\eta \rightarrow 0$, $f_{\alpha_1 \alpha_2} \sim A_1 \eta^{-\alpha_1} + A_2 \eta^{-\alpha_2}$, and when $\alpha_1 = \alpha_2 = \alpha$, $f_{\alpha \alpha} \sim (A - B \ln \eta) \eta^{-\alpha}$. A means of testing this result experimentally is indicated when $M = m_\pi$.

In Sec. 4, the Reggeon triangle graph is discussed. Gribov's⁸ rules are found to apply provided that certain extra factors are included. Because of these, the Reggeon "Ward identity" suggested by Anselm and Dyatlov⁹ no longer holds.

The analytic structure of the double partial-wave amplitude corresponding to the triangle is investigated. In addition to the usual two-Reggeon cuts correspond-

ing to contractions, there is also a leading curve corresponding to the uncontracted diagram. The curve bears a relationship to the two-Reggeon branch points similar to that of an anomalous threshold to normal thresholds. In particular, it touches the two-Reggeon branch points.

The asymptotic behavior of the production amplitude turns out to be controlled by the leading curve. It has the form $T \sim s^J / \ln s$, where the exponent J depends on $q_3'^2$ as well as on $q_1'^2$ and $q_2'^2$. This is quite different from the type of behavior that emerges from double-Reggeon

exchange and has no analog in two-body scattering. The identification of such behavior experimentally would be an important support for the relevance of a Reggeon calculus.

Finally, it was noted that a necessary condition for the appropriateness of the definition adopted in this paper for the multi-partial-wave amplitude is the asymptotic simplicity of the analytic structure of the production amplitude. Such simplicity does seem to emerge from Gribov's analysis applied to production amplitudes.

Two-Boson-Exchange Effects in Nucleon-Nucleon Scattering

RICHARD D. HARACZ

Drexel Institute of Technology, Philadelphia, Pennsylvania 19104

AND

RAVI D. SHARMA*

Temple University, Philadelphia, Pennsylvania

(Received 17 June 1968)

The two-pion-exchange contribution to nucleon-nucleon scattering is studied at scattering energies of 95 and 310 MeV through a partial-wave analysis of the exact relativistic scattering matrix. Additional two-boson-exchange effects are also studied at these energies corresponding to the $\pi+\eta$ and $\pi+\sigma$ exchange processes, with η the pseudoscalar resonance and σ the scalar resonance. It is found that the two-pion-exchange (TPE) phase parameters are large compared with one-pion-exchange (OPE) phase parameters for low values of L , and OPE+TPE is a reasonable representation of the phenomenological phases for the lower energy when $L \geq 3$ and for the higher energy when $L \geq 5$. The $\pi+\eta$ effect is found to be small compared with the pion-theoretical effects, but the $\pi+\sigma$ effect is large for a light scalar resonance if it couples strongly with the nucleon.

1. INTRODUCTION

THE description of the nucleon-nucleon interaction by resonance models consists of some compensation for the core of the interaction and contributions from the virtual exchange of a single π meson, an η pseudoscalar resonance, the ω and ρ vector resonances, and scalar resonances.¹ Despite the fact that the two-pion-exchange (TPE) mass is less than any established resonance mass, resonance models either exclude the TPE effect or simulate it by some approximation—perhaps by the introduction of scalar resonances whose existences have not yet been conclusively

established experimentally. Moreover, the effect of the virtual exchange of a pion and η resonance together has not been considered even though the mass exchanged is less than a single vector resonance mass. Finally, if a light scalar resonance σ is used in a resonance model, the $\pi+\sigma$ effect should also be considered. It would therefore seem of interest to evaluate the TPE, $\pi+\eta$, and $\pi+\sigma$ contributions to nucleon-nucleon scattering.

An exact determination of the relativistic scattering operator for nucleon-nucleon scattering due to two-pion exchange by Gupta has been available since 1960.² It includes the total contribution of the pion-nucleon pseudoscalar interaction through the fourth order in the pion-nucleon coupling constant. A nonrelativistic approximation is also presented from which a potential is derived, and by using this potential Breit *et al.*³ obtained two-pion-exchange phase parameters.

In a later work, Gupta, Haracz, and Kaskas obtained the relativistic scattering matrix corresponding to the TPE scattering operator and evaluated it at nucleon

* Present address: Bellcomm Inc., Washington, D. C. 20024.

¹ R. A. Bryan and G. L. Scott, Phys. Rev. **135**, B434 (1964); A. E. S. Green and R. D. Sharma, Phys. Rev. Letters **14**, 390 (1965); A. Scotti and D. Y. Wong, Phys. Rev. **138**, B145 (1965); J. S. Ball, A. Scotti, and D. Y. Wong, *ibid.* **142**, 1000 (1966); R. A. Bryan and R. A. Arndt, *ibid.* **150**, 1299 (1966); R. A. Arndt, R. A. Bryan, and M. H. MacGregor, *ibid.* **152**, 1490, (1966); A. E. S. Green, T. Sawada, and R. D. Sharma, *Isobaric Spin In Nuclear Physics* (Academic Press Inc., New York, 1966); R. A. Bryan and B. L. Scott, Phys. Rev. **164**, 1215 (1967); R. D. Sharma and A. E. S. Green, Nucl. Phys. **B3**, 33 (1967). These references may be consulted for additional work on resonance models.

² S. N. Gupta, Phys. Rev. **117**, 1146 (1960).

³ G. Breit, K. E. Lassila, H. M. Ruppel, and M. H. Hull, Jr., Phys. Rev. Letters **6**, 138 (1961).